Two-dimensional nonlinear optically-induced photonic lattices in photorefractive crystals

Anton S. Desyatnikov[a], Dragomir N. Neshev[a], Robert Fischer[a], Wieslaw Krolikowski[b], Nina Sagemerten[c], Denis Träger[c], Cornelia Denz[c], Alexander Dreischuh[d], and Yuri S. Kivshar[a]

[a] Nonlinear Physics Center and [b] Laser Physics Center, Center for Ultra-high bandwidth Devices for Optical Systems (CUDOS), Research School of Physical Sciences and Engineering, Australian National University, Canberra ACT 0200, Australia
[c] Institute of Applied Physics, Westfälische Wilhelms-Universität Münster D-48149 Münster, Germany
[d] Department of Quantum Electronics, Sofia University, BG-1164 Sofia, Bulgaria

ABSTRACT

We study theoretically and generate experimentally two-dimensional nonlinear optically-induced photonic lattices with periodic phase modulation of different geometries in a photorefractive medium, including the periodic nonlinear waves with an internal energy flow or vortex lattices. We demonstrate that the light-induced periodically modulated nonlinear refractive index is highly anisotropic and nonlocal, and it depends on the orientation of a two-dimensional lattice relative to the crystal axis. We discuss stability of such optically-induced photonic two-dimensional structures and demonstrate experimentally their waveguiding properties.

Keywords: Photorefractive medium, nonlinear waves, soliton arrays, optically-induced photonic lattices

1. INTRODUCTION

The study of nonlinear effects in periodic photonic structures recently attracted strong interest because of many novel possibilities to control light propagation, steering and trapping. Periodic modulation of the refractive index modifies the linear spectrum and wave diffraction and consequently strongly affects the nonlinear propagation and localization of light, including the formation of novel types of self-trapped optical beams, spatial solitons.[1]

Photonic lattices can be induced optically by *linear* diffraction-free light patterns created by interfering several plane waves.[2] However, the induced change of the refractive index depends on the light intensity and, in the nonlinear regime, it is accompanied by the self-action effect.[3] The nonlinear diffraction-free light patterns in the form of stable self-trapped nonlinear periodic waves can propagate without change in their profile, becoming the eigenmodes of the self-induced periodic potentials. This behavior is generic, since *nonlinear periodic waves* can exist in many types of nonlinear systems, and they provide a simple realization of *nonlinear photonic crystals*.[4] Such structures can be considered as flexible because the lattice is modified and shaped by the nonlinear medium. Such flexible nonlinear photonic lattices extend the concept of optically-induced gratings beyond the limits of weak material nonlinearity. Moreover, the nonlinear lattices offer many novel possibilities for the study of nonlinear effects in periodic systems because they can interact with localized signal beams via the cross-phase modulation and can form a composite bound states.[5,6]

Nonlinear photonic lattices created by two-dimensional arrays of *pixel-like* spatial solitons have recently been demonstrated experimentally in parametric processes,[7] and in photorefractive crystals with both coherent[8] and partially incoherent[3,6,9] light. For the case of two-dimensional arrays of *in-phase* spatial solitons created by the amplitude modulation, every pixel of the lattice induces a waveguide which can be manipulated by an external steering beam.[8–10] However, the spatial periodicity of these two-dimensional soliton lattices is limited by the

WWW addresses: [a] www.rsphysse.anu.edu.au/nonlinear, [b] www.uni-muenster.de/Physik/AP/Denz

Tenth International Conference on Nonlinear Optics of Liquid and Photorefractive Crystals, edited by Gertruda V. Klimusheva, Andrey Iljin, Sergey Al. Kostyukevych, Proc. of SPIE Vol. 6023, 60230H, (2005) · 0277-786X/05/$15 · doi: 10.1117/12.648200

attractive soliton interaction that may leads to their strong instability. In contrast, the recently suggested two-dimensional square lattices created by *out-of-phase* spatial solitons are known to be robust in isotropic saturable model.[11] The phase profile of such self-trapped waves resembles a chessboard pattern with the lines of π-phase jumps between neighboring white and black sites. Recently, we suggested both theoretical and experimental approaches for generating this type of two-dimensional nonlinear lattices in anisotropic photorefractive media.[12] We also identified two distinct types of square lattices, square and diamond patterns, emerging as a consequence of anisotropy, i.e. for different orientations of the symmetry axes of the lattice with respect to photorefractive crystal c-axis.

In this paper, we summarize our recent results on the theoretical and experimental study of two-dimensional nonlinear optically-induced photonic lattices in photorefractive crystals. First, we study theoretically, using an anisotropic nonlocal model of photorefractive nonlinearity, the spatial phase-modulated two-dimensional structures in self-focusing nonlinear media. We introduce novel types of two-dimensional nonlinear modes, including triangular lattices of two different orientations, and square and hexagonal lattices with phase dislocations. The square vortex lattice has a square-like symmetry of the intensity distribution, while the hexagonal intensity pattern is build with the honeycomb structure of vortices. In experiment, we generate these new types of self-trapped two-dimensional nonlinear waves and study their waveguiding properties. In particular, we demonstrate that the light-induced periodically modulated nonlinear refractive index is highly anisotropic and nonlocal, and it depends on the lattice orientation relative to the crystal axis.

An advantage of using this novel type of nonlinear periodic lattices when compared with in-phase lattices or incoherent soliton arrays[3,8] is that such lattices can be made robust even with smaller lattice spacing. This creates an opportunity for experimental studies of mutual coupling of periodic and localized waves recently discussed for one-dimensional geometry, as well as the generation of two-dimensional composite lattice solitons.[5] Remarkably stable *hexagonal* pattern with nested honeycomb lattice of vortices is demonstrated experimentally for spatial period of intensity distribution approximately equals to 22μm, the lowest ever reported periodicity for the nonlinear self-trapped waves.

The paper is organized as follows. In Section 2, we describe our theoretical model and introduce several types of two-dimensional nonlinear structures as self-trapped solutions of those equations. Our experimental results are presented in Section 3, where we describe our experimental approach and summarize our results for the two-dimensional lattices with nontrivial vortex-like phase patterns. Section 4 summarizes our paper.

2. THEORETICAL APPROACH

Spatially periodic nonlinear modes appear naturally due to the self-focusing effect and modulational instability.[1] When self-focusing effect compensates for diffraction of optical beams, it may support both isolated spatial solitons and periodic soliton trains. The latter can be identified as stationary periodic nonlinear waves, and they include well studied *cnoidal waves*, described by the *cn* and *dn* Jacobi elliptic functions as the stationary solutions of the generalized nonlinear Schrödinger (NLS) equation,[1]

$$i\frac{\partial E}{\partial z} + \frac{\partial^2 E}{\partial x^2} + n(I)E = 0, \tag{1}$$

where $I \equiv |E|^2$. Similar nonlinear waves appear as periodic solutions of other nonlinear models, including the familiar models of quadratic and Kerr-type saturable nonlinearities. The family of two-dimensional nonlinear periodic waves[11] can also be extended to describe the case of the rectangular geometry with two different transverse periods, because such anisotropic deformations of the square lattice do not enhance its modulational instability. Stabilization of phase-engineered soliton arrays was reported recently for the case of an anisotropic nonlinear model.[10]

In this paper, we study two-dimensional optically-induced lattices in a photorefractive crystal known as an example of anisotropic and nonlocal nonlinear media. In this case, the nonlinear contribution to the refractive index in the model (1) is given by[13]

$$n(I) = \sigma\Gamma\frac{\partial\varphi}{\partial x}, \tag{2}$$

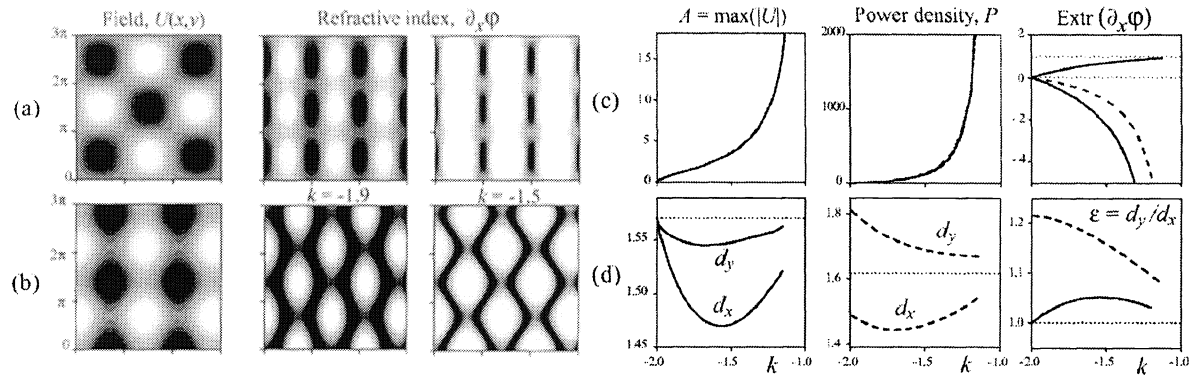

Figure 1. (a) Square and (b) diamond self-trapped stationary periodic patterns in the model (1)-(3) at $\Gamma = 1$. Families of nonlinear waves are summarized in (c) and (d); solid (dashed) lines correspond to the square (diamond) patterns. Both lines for A, P, and $\max(\partial_x\varphi)$ coincide in (c). Horizontal dotted lines in (d) correspond to the linear limit $\Gamma \to 0$.

where the parameter $\Gamma = x_0^2\kappa^2 n_0^2 r_{\text{eff}}\mathcal{E}$ is defined through the effective electro-optic coefficient r_{eff} and externally applied bias electrostatic field $\mathcal{E}$. The dimensionless parameter $\sigma = \pm 1$ indicates the polarity of applied voltage changing the character of photorefractive screening nonlinearity: self-focusing for $\sigma = +1$, and self-defocusing otherwise.

The electrostatic potential φ of the optically-induced space-charge field satisfies a separate equation:

$$\nabla_\perp^2\varphi + \nabla_\perp\varphi\nabla_\perp \ln(1+I) = \frac{\partial}{\partial x}\ln(1+I), \tag{3}$$

where, for simplicity, we use the standard notation $\nabla_\perp$ for the two-dimensional gradient operator such that

$$\nabla_\perp^2 = \frac{\partial^2}{\partial x^2} + \frac{\partial^2}{\partial y^2},$$

and the intensity I is measured in units of the background illumination (dark) intensity, necessary for the formation of spatial solitons in such a medium. The physical variables $\tilde{x}$, $\tilde{y}$, and $\tilde{z}$ correspond to their dimensionless counterparts as $(\tilde{x},\tilde{y}) = x_0(x,y)$ and $\tilde{z} = 2\kappa x_0^2 z$, here x_0 is the transverse scale factor and $\kappa = 2\pi n_0/\lambda$ is the carrier wave vector with the linear refractive index n_0.

Stationary solutions to the system (1)-(3) are sought in the standard form, $E(x,y,z) = U(x,y)\exp(ikz)$ where the real envelope U satisfies the equation

$$-kU + \nabla_\perp^2 U + \Gamma U\frac{\partial\varphi}{\partial x} = 0. \tag{4}$$

Following the Ref.,[12] we first look for periodic solutions of square geometry, $U(X,Y) = U(X+2\pi, Y+2\pi)$, and solve Eqs. (3), (4) using the relaxation technique[13] with initial ansatz in the form of a linear periodic mode, $U_{\text{lin}}(X,Y) = A\sin X\,\sin Y$. We find that at least two distinct families bifurcate from the linear wave $U_{\text{lin}}(X,Y)$, depending on its orientation: a square pattern parallel to the c -axis with $X = x$ and $Y = y$, and a diamond pattern oriented diagonally, in the latter case $X = (x+y)/\sqrt{2}$ and $Y = (x-y)/\sqrt{2}$. Figures 1(a) and 1(b) show the field and refractive index distributions in the low ($k = -1.9$, $A \simeq 0.9$) and relatively high ($k = -1.5$, $A \simeq 3.6$) saturation regimes for both families. In a general case $\Gamma \neq 1$, these two families occupy a band $k \in [-2, \Gamma - 2]$ with the amplitudes $A(k)$ and power densities $P(k)$ vanishing in the linear limit $k \to -2$, see Fig. 1(c). Here the power density is defined as the power of a unit cell, $P = 4\int\int_0^\pi U^2 dXdY$. The main difference between two solutions, clearly seen in Figs. 1(a) and 1(b), comes from the refractive index: the regions with the effective focusing lenses are well separated for the diamonds, and fuse to the effectively one-dimensional stripes for square

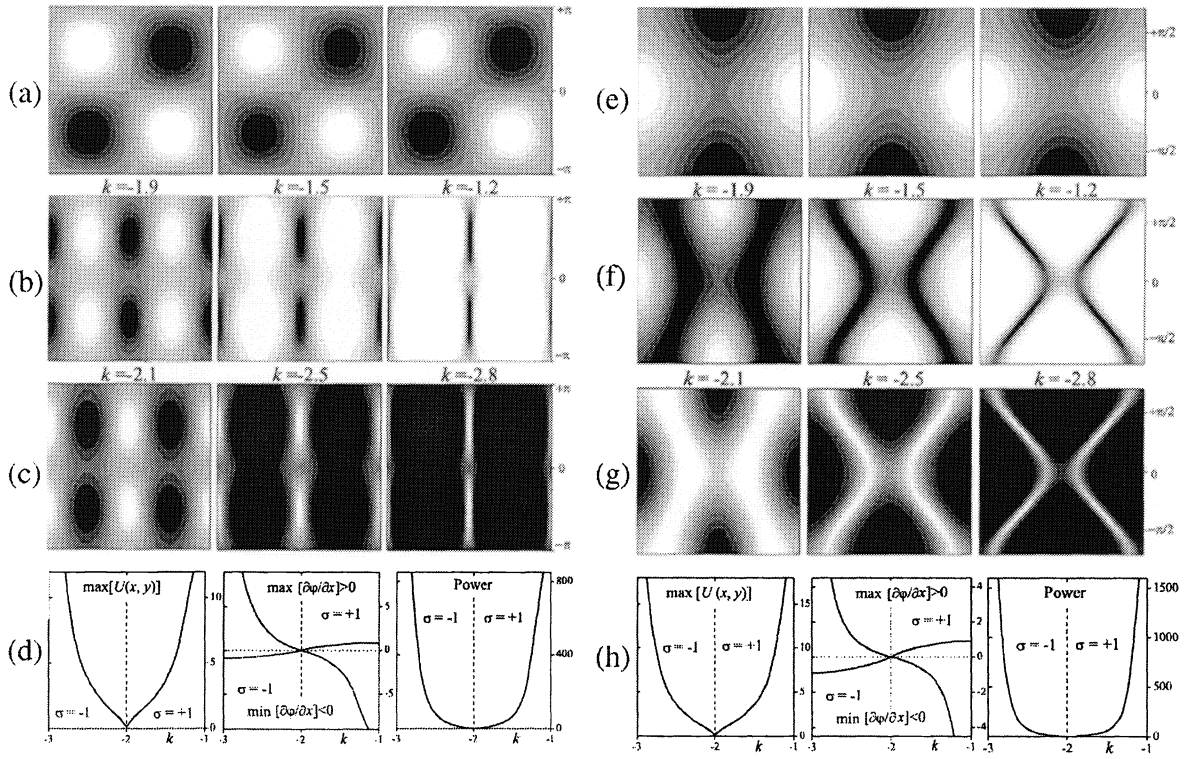

Figure 2. Comparison between elementary cells and families of the square (a-d) and diamond (e-h) patterns in self-defocusing [$\sigma = -1$, (b,f)], and self-focusing [$\sigma = +1$, (g,h)] media. Field [$U(x, y)$ in (a,e)] and refractive index [$\partial_x \varphi$ in (b,c,f,g)] distributions are shown for three distinct values of amplitude $A = \max[U(x, y)]$, or propagation constant k, from low (left) to high (right) saturation.

pattern, in the limit of strong saturation. In Fig. 1(c), we plot maximal and minimal values (extrema) of the refractive index, $\mathrm{Extr}(\partial\varphi/\partial x)$.

In Fig. 1(d) we show the FWHM of a single intensity spot in two orthogonal directions, $d_{x,y}$, characterizing the degree of spatial localization of cnoidal wave.[11] The ellipticity of every lattice site, $\varepsilon = d_y/d_x \geq 1$, depends on the propagation constant k, similar to the ellipticity of a single photorefractive soliton,[13] see Fig. 1(d).

The model (1-3) includes the self-defocusing nonlinearity which can be realized with reversing the polarity of a bias external filed applied to photorefractive medium. In this case, we also found numerically the stationary periodic waves similar to the shown in Fig. 1, namely the square periodic waves, the two-dimensional analog of the *sn*-type one-dimensional cnoidal waves. Corresponding families of such solutions are compared to the square patterns in self-focusing medium in Fig. 2. Note that, while the field distribution is almost identical in both cases, the refractive index is opposite: the positive maxima in self-focusing case (focusing lenses) is inverted for $\sigma = -1$ and represent defocusing lenses (induced potential maxima). Due to the nonlocality here appear sharp potential minima in strong saturation limit (white lines in right frames in Figs. 2(c,g)). The study of the guiding properties of these types of induced photonic structures is currently in progress. Note that the parameters of two families for $\sigma = \pm 1$ in Figs. 2(d,e) are almost symmetric with respect to linear solution $k = -2$, however, two families occupy different bands.

In order to test stability of the square lattice, we propagate numerically two types of initially perturbed periodic solutions and observe robust propagation for the distances exceeding the experimental crystal length. Figure 2 (a,b) demonstrates an example of a stable propagation for the parameters close to our experimental situation. We compare these pictures with experimental results, obtained as described in the following section.

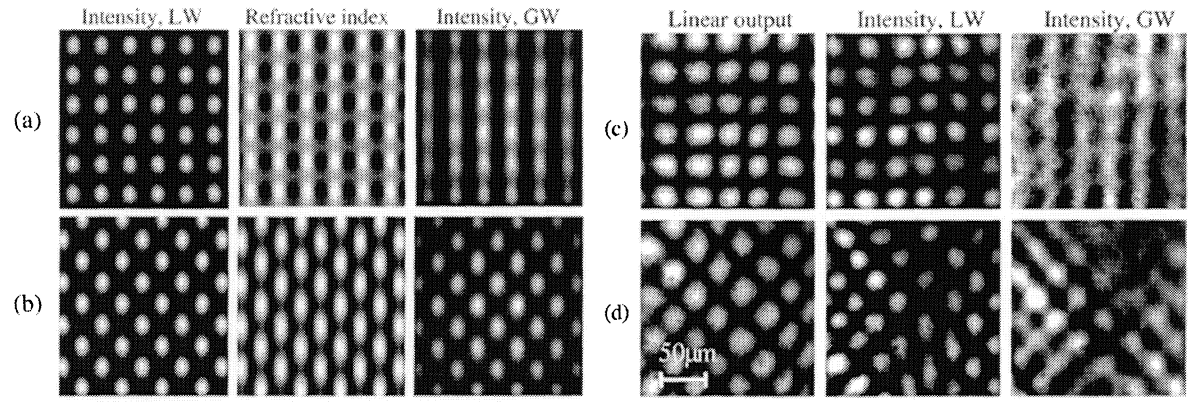

Figure 3. Numerical results for the propagation of (a) square and (b) diamond self-trapped patterns for $\Gamma = 11.8$ in the low saturation regime $A \approx 1$, $k = -0.5$. Intensities of the lattice and probe wave it guides are shown after propagation $\tilde{z} \approx 23$ mm. On the input, the lattice is perturbed with 20% of random noise, and the probe is a broad Gaussian beam. Experimental results for the (c) square and (d) diamond lattices. Left to right: output intensities of the lattice after linear and nonlinear propagation, and output of a guided plane wave, respectively.

3. EXPERIMENTAL RESULTS

To demonstrate experimentally both the existence and stability of the nonlinear periodic lattices generated in anisotropic and nonlocal photorefractive media, we use an experimental setup similar to that employed earlier.[12] In this arrangement, a linearly polarized beam from a frequency-doubled cw Nd:YVO_4 laser at 532 nm is sent to a liquid crystal programmable spatial light modulator (SLM) Hamamatsu X8267, in order to create a periodic light pattern with a variable period and orientation. The output of the modulator is then imaged by a high numerical aperture telescope on to the front face of a 2 cm long photorefractive SBN:60 crystal. The polarization of the beam is parallel to the c-axis, thus experiences strong photorefractive nonlinearity. The modulator imposes pure phase modulation onto the beam, which transforms into an amplitude modulation at the front face of the crystal, where noise is reduced by proper spatial filtering. The crystal is externally biased and uniformly illuminated with a white-light to control the dark irradiance. The generated periodic pattern represents a non-diffracting periodic wave, and it experiences robust linear propagation inside the crystal (at zero bias). The input of the generated periodic wave, therefore will be identical to the linear output. The specific geometric and the lattice structures are discussed below.

3.1. Lattices with edge-type phase modulation

A typical example of the intensity pattern at the back face of the crystal is shown in Fig. 3 (c,d) for two different orientations with respect to the crystal axis.[12] Since the neighboring lattice sites are out-of-phase (edge-type phase dislocation between them), they do not exchange energy. Because of this, it is expected that such type of lattice will alow to decrease substantially the lattice period with respect to the nonlinear lattices of closely spaced in-phase solitons. Indeed the presented example shows that the lattice propagates stably for periodicity of 31 μm, which is twice less than the smallest generated coherent in-phase soliton array. Besides of inhomogeneities in the periodic pattern, the experimental pictures are in a good agreement with the corresponding numerical simulations presented in Fig. 3 (a,b). To test the induced periodic refractive index modulation inside the crystal we tested the guiding of a plane wave inside the nonlinear optical lattice. The observed guided pattern is shown in Fig. 3 (c,d-right column), and demonstrate the qualitative difference of the induced refractive index modulation for two different orientations of the lattice. In the case of a square pattern oriented along the principal axis of the crystal the induced refractive index change is almost one-dimensional - the horizontal modulation is much stronger than the modulation along the vertical direction. In the case of diagonal orientation - diamond pattern, the modulation is fully two-dimensional.

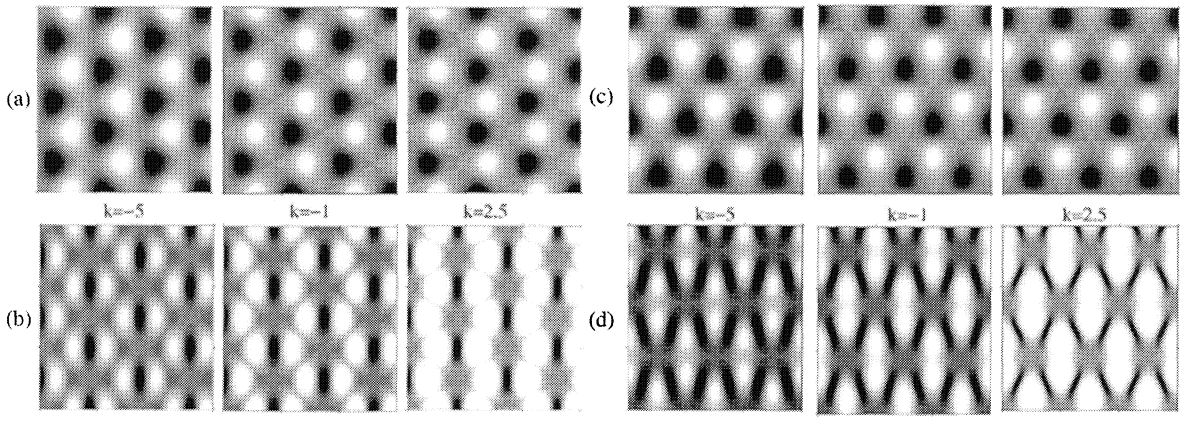

Figure 4. Families of triangular lattices in self-focusing media. Field (a,c) and refractive index (b,d) for the three different intensities (three different soliton parameter values $k = -5, -1, 2.5$) and two different orientation: perpendicular in (a,b) and parallel in (c,d).

Another type of edge-type phase modulated nonlinear lattices is the triangular pattern depicted theoretically in Fig. 4. We traced two distinct families of such stationary solutions in photorefractive model, the one with common lines of phase jump perpendicular to the c -axis shown in Fig. (4) (a,b), and the triangular lattice with parallel orientation, Fig. 4 (c,d). In the latter case the two-dimensional refractive index pattern, e.g. in the Fig. 4(d) (right), is very similar to the diamond lattice (see Fig. 1(b)), with that difference, that each refractive index hump (effective waveguide) is created by the dipole-mode, i.e. bound state of two out-of-phase sites (cf. the field distributions in Fig. 1(b) and Fig. 4(d)). Therefore, the triangular lattice with parallel orientation can be seen as the higher-order generalization of the diamond pattern. Experimental investigation of these type of lattices is currently on the way.

3.2. Vortex-like lattices

Expanding the idea of phase-modulated self-trapped waves we introduce the *vortex lattices*. Theoretically, these nonlinear waves bifurcate from corresponding linear solutions, easily found from linear paraxial Eq. 1 with $n(I) = 0$. For example, it is well known that the linear superposition of two azimuthal modes $\cos\varphi$ and $\sin\varphi$, with azimuthal coordinate φ, gives rise to the vortex beam with phase dislocation $\exp(i\varphi)$. Similarly, superimposing two linear modes U_{lin} (see above), we obtain the square vortex lattice, $U_{\text{vortex}} = A\{\sin x \sin y + i \cos x \cos y\}$. Family of nonlinear solutions, which bifurcate from U_{vortex}, is depicted in Fig. 5 (a,b).

Experimentally, we generate a square-type vortex lattice, oriented diagonally to the principal axis of the crystal with a large period of 57 μm. In this type of pattern the relative phase between the lattice sites is $\pi/2$ and in between the lattice sites there is a vortex-type phase dislocation. Due to the phase difference between the lattice sites they do exchange energies even for very large lattice periods. Such a pattern also represents a non-diffracting linear wave and indeed propagated without change in for zero applied biasing voltage. Applying an external DC electric field ($\mathcal{E}$=1300 V/cm) across the crystal provides appropriate conditions for the formation of spatial solitons of $\sim$15 μm size. Such a voltage will also influence the propagation of the periodic wave. At this high voltage (nonlinearity), however, the output of the lattice does not change significantly [Fig. 5(c) (left column)] and the position of the vortices is generally preserved [Fig. 5(c) (inset)]. This is due to the fact that the profile of the nonlinear periodic solution is fairly close to the linear non-diffracting wave.

In order to test that the lattice indeed propagates truly nonlinearly, we probed the induced changes to the crystal refractive index. To do this, we sent a broad plane-wave trough the crystal and observed its modulation at the output. In practice, this is realized by switching-off the voltage on the phase modulator, thus removing the modulation imposed on the light pattern and generating a broad plane-wave of desired orientation at the input of the crystal. We than reprogrammed the SLM such that the plane wave is propagating exactly along the

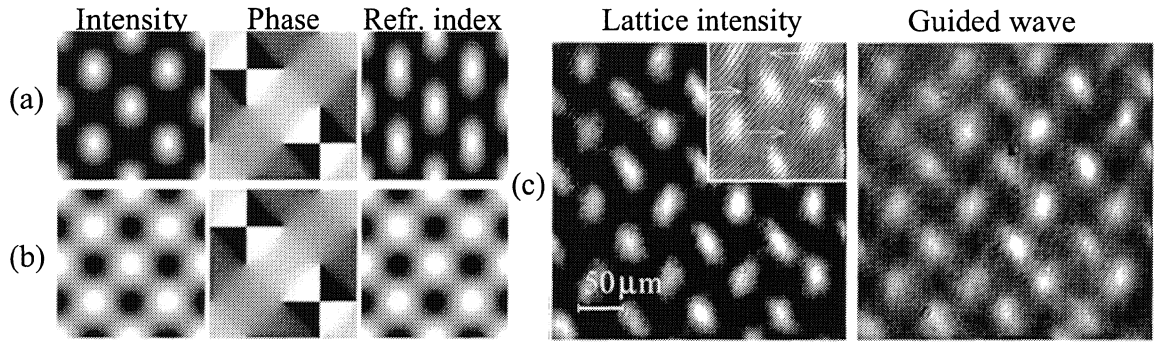

Figure 5. Diagonally-oriented square vortex lattices in self-focusing media: (a,b) Numerically calculated family of solution. Solutions are shown for $\Gamma = 11.8$ (a) close to linear diffraction-free wave for $k = -0.1$, and for high saturation $k = -0.49$ (b). (c) Experimentally observed example of vortex lattice of a period 57 μm: Left - nonlinear output for bias 1.3kV; Inset - interference with a reference broad beam to monitor the position of the vortex-type dislocations (marked by arrows); Right - guided plane wave through the induced index modulation launched at the middle of the Brillouin zone.

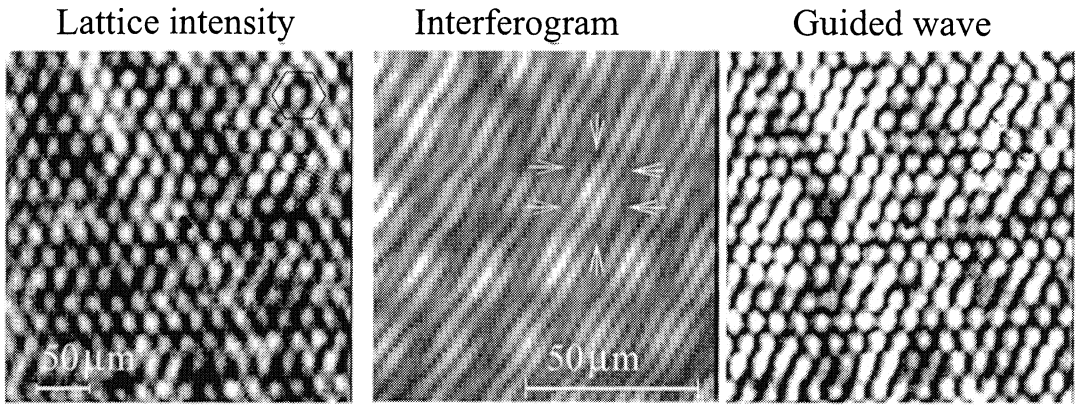

Figure 6. Experimentally observed hexagonal vortex lattice of a period 22 μm. Left: Nonlinear output for bias 1.3kV; Middle - magnified part of the bottom right part of the lattice with interference with a reference beam to identify the position of the vortices (marked by arrows); Right - plane wave modulated by the induced index modulation launched at the edge of the Brillouin zone.

induced waveguides, e.g. in the middle of the first Brillouin zone. Due to the slow response of the photorefractive crystal, we can quickly monitor the output of the plane wave without modifying the induced refractive index change. Output intensity distributions for two orientations of the lattice pattern are shown in Fig. 5(c) (right column). As clearly seen, the plane-wave is indeed modulated by the induced periodic potential, and we observed guiding of the probe beam at the maxima of the refractive index. This experimental observation is in a good agreement with the corresponding numerical simulations [Fig. 5(a,b)].

The idea of generating vortex lattices as non-diffracting linear waves can be further extended in more complex geometries such as hexagonal lattices shown in the experimental Figure 6. In this type of pattern the lattice sites are situated in a hexagonal, closely packed lattice, while the vortex-type dislocations are situated in a honeycomb lattice of a smaller spacing. Even though the vortices in the lattice are very closely packed, we demonstrated that such type of lattice can be experimentally generated and observed for rather small lattice periods, as shown in Fig. 6 (left column) for a period of 22 μm. The position of the vortices is also preserved as seen in Fig. 6 (middle column). In order to probe the refractive index modulation we send a plane wave trough the crystal (by fast reprogramming of the modulator) and directed it at the edge of the Brillouin zone in order to test the

bang-gap structure of the induced lattice. This type of test allows not only to probe the periodic modulation, but additionally to test the inhomogeneities of the periodic pattern, since the gap in the the transmission spectrum is strongly dependent on structural defects and disorder. In this experimental test, at the output of the crystal we observed a strong periodic modulation of the output wave, with the maxima of the pattern located in between the lattice sites. This indicates a strong excitation of the Bloch waves corresponding to the second transmission band. This observation proves that the induced nonlinear vortex lattice is indeed stable and with good spatial homogeneity.

4. CONCLUSIONS

We have studied theoretically and generated experimentally two-dimensional nonlinear optically-induced photonic lattices in photorefractive crystals. With the help of a nonlocal anisotropic nonlinear model, we have described two distinct classes of self-trapped spatially-periodic nonlinear lattices with out-of-phase neighboring sites, the square pattern oriented parallel to the crystal axes, and the diamond pattern oriented diagonally in the transverse plane. We have demonstrated that the highly anisotropic refractive-index distribution induced by the lattice differs significantly from its isotropic counterpart and depends strongly on the lattice orientation.

ACKNOWLEDGEMENTS

This work was initiated by a visit of Dr. Dragomir Neshev to the University of Münster, supported by the Australia-Germany Exchange Program of the Australian Academy of Science. The work was also supported by the Australian Research Council and the Alexander von Humboldt Foundation.

REFERENCES

1. Yu. S. Kivshar and G. P. Agrawal, *Optical Solitons: From Fibers to Photonic Crystals* (Academic, San Diego, 2003), 540 pp.; and references therein.
2. J.W. Fleischer, M. Segev, N. K. Efremidis, and D. N. Christodoulides, Nature **422**, 147 (2003).
3. Z. Chen, and K. McCarthy, Opt. Lett. **27**, 2019 (2002).
4. S.F. Mingaleev, Yu.S. Kivshar, and R. Sammut, in: *Soliton-driven Photonics*, A.D. Boardman and A.P. Sukhorukov, Eds. (Kluwer, Dordrecht, Netherlands, 2001), pp. 487-504.
5. A. S. Desyatnikov, E. A. Ostrovskaya, Yu. S. Kivshar, and C. Denz, Phys. Rev. Lett. **91**, 153902 (2003).
6. D. Neshev, Yu. S. Kivshar, H. Martin, and Z. G. Chen, Opt. Lett. **29**, 486 (2004).
7. S. Minardi, S. Sapone, W. Chinaglia, P. Di Trapani, and A. Berzanskis, Opt. Lett. **25**, 326 (2000).
8. J. Petter, J. Schröder, D. Träger, and C. Denz, Opt. Lett. **28**, 438 (2003).
9. H. Martin, E. D. Eugenieva, Z. Chen, and D. N. Christodoulides, Phys. Rev. Lett. **92**, 123902 (2004).
10. M. Petrovič, D. Träger, A. Strinič, M. Belič, J. Schröder, and C. Denz, Phys. Rev. E **68**, 055601R (2003).
11. Ya. V. Kartashov, V. A. Visloukh, and L. Torner, Phys. Rev. E **68**, 015603 (2003).
12. A. S. Desyatnikov, D. N. Neshev, Y. S. Kivshar, N. Sagemerten, D. Träger, J. Jägers, C. Denz, and Y. V. Kartashov, *Nonlinear photonic lattices in anisotropic nonlocal self-focusing media*, Opt. Lett., in press.
13. A. A. Zozulya, D. Z. Anderson, A. V. Mamaev, and M. Saffman, Phys. Rev. A **57**, 522 (1997).
14. Z. Chen, H. Martin, E. D. Eugenieva, J. Xu, and A. Bezryadina, Phys. Rev. Lett. **92**, 143902 (2004).